Journal of Power Sources 240 (2013) 26–32

Contents lists available at SciVerse ScienceDirect

Journal of Power Sources

journal homepage: www.elsevier.com/locate/jpowsour

Design of novel charge balancing networks in battery packs

D. Dane Quinn [a,*], Tom T. Hartley [b]

[a] Department of Mechanical Engineering, The University of Akron, Akron, OH 44325-3903, USA
[b] Department of Electrical and Computer Engineering, The University of Akron, Akron, OH 44325-3904, USA

HIGHLIGHTS

- We consider the performance of charge balancing systems for multi-cell battery packs.
- The performance is measured by the voltage equalization rate and the steady-state cell unbalance.
- The performance depends on the topology of the cell-to-cell connections.
- The performance can be correlated with graph theoretic properties of the underlying network.

ARTICLE INFO

Article history:
Received 25 October 2012
Received in revised form
13 March 2013
Accepted 24 March 2013
Available online 9 April 2013

MSC:
83.06
83.14
83.15
190.060

Keywords:
Batteries
Charge balancing
Graph theory
Mathematical modeling

ABSTRACT

In a modern battery pack, the charge in the individual cells can diverge in time, leading to decreased capacity and reduced operating life of the pack. Charge balancing systems can be introduced to equalize the state of charge across the multiple cells, therefore increasing the performance of the battery pack. This work considers the dynamic performance of charge balancing systems, and through simulation explores how their ability to equalize the state of charge depends on the design of the underlying charge balancing network. The performance of the charge balancing system is described in terms of the rate at which the individual cells converge and the maximum cell voltage deviation in the pack. Specifically the performance of the charge balancing system is shown to correlate with graph theoretic properties of the underlying charge balancing network, including the diameter and spectral gap. Several different underlying charge balancing networks are considered, applied to an 8-cell pack, with two parallel strings of four cells in series.

1. Introduction

Modern battery packs are composed of multiple cells, combined to achieve required voltage and current levels. Four main networks can be identified that allow for individual cells to interact with one another; the power network, the communication network, the balancing network, and the safety network. The power network transfers energy from the individual cells in the pack, through the pack terminals, and into an attached load. The communication network transfers information about each of the cells throughout the pack, and often to a pack manager and a user information console. The balancing network transfers charge throughout the pack to maintain a balanced state-of-charge among the individual cells (or a balanced state-of-energy). Finally, the safety network carries pack reconfiguration information throughout the pack, allowing for the restructuring of the pack when a fault condition is detected. Clearly, each of these networks requires specific hardware to accomplish its task, however varying degrees of functionality compete with complexity and cost in the construction of a real pack. Thus every pack trades off the functionality of each topology with its cost. The purpose of this paper is to provide a framework for the understanding and design of cell balancing networks, and how their topology influences the ability of the pack to achieve a balanced state.

Ideally each individual cell in a battery pack has identical characteristics, so that they all react identically to various stimuli. However, in practice the individual cell characteristic parameters vary from cell to cell due to, for example, manufacturing differences,

* Corresponding author. Tel.: +1 330 972 6302.
E-mail addresses: quinn@uakron.edu (D.D. Quinn), thartley@uakron.edu (T.T. Hartley).

0378-7753/$ – see front matter © 2013 Elsevier B.V. All rights reserved.
http://dx.doi.org/10.1016/j.jpowsour.2013.03.113

environmental conditions such as localized temperature in the pack, or an evolving damage state of the cell. Some cells will have increased self-discharge rates. Some will have higher voltages due to their temperature. Some will have higher internal resistances causing voltage variation and heating. In nearly every battery pack, individual cell characteristics will diverge from those of the other cells in their pack. Historically, with lead and nickel based chemistries, the cells could be brought into balance by overcharging the full cells while the continuing to charge cells that had yet to reach their charge capacity. Major damage in the full cells was avoided by reducing the overall pack current as the pack voltage reached some predetermined level. Unfortunately, the modern lithium based chemistries do not allow overcharging of individual cells without significantly shortening their useful life. Thus, some form of cell balancing is usually required for lithium based chemistries [1–5].

To overcome this scenario, a charge balancing system can be introduced, whereby charge is shuttled from one cell to another to balance the state of charge across the pack [6–8]. Balancing in the charging cycle is often accomplished by using bypasses. When a cell is approaching a full state, a current bypass is often turned on to reduce the current flowing to the cell. The diverted current is usually passed through a resistor where the energy is converted to heat. Thus, this method can result in significant energy inefficiency and is only active during the charging sequence.

Another approach to balancing is the use of a flying capacitor [9]. This capacitor requires switches to connect its terminals to the terminals of every cell in the pack. The capacitor can then take charge from high voltage cells, and transfer it into low voltage cells. A problem with this approach is the serious decrease in pack reliability due to the possible failure of the large number of switches. Another problem is the heating of the switches when they close due to large voltage mismatches and thus high currents. Yet another problem is that only one charge transfer can occur at a time if only one flying-capacitor is used. These concerns also apply to strings of parallel flying-capacitors, as well as DC–DC converter structures using many parallel inductors.

The third main approach to balancing is the use of transformers. Some multi-transformer based balancers will take energy from individual cells, and then place it back into the entire pack where it is distributed among all the cells. Another approach is to use a two-terminal transformer to take charge from an individual cell, and to place it into another individual cell [6–8]. This approach has the benefit of having all the cells electrically isolated from all the others, as the energy is transferred through magnetic fields in the transformer cores. Another benefit is that all of the transformers can be engaged simultaneously. However, the charge balancing system is limited by the number of connections between cells. For a pack with N total cells, the number of connections required to connect each cell to every other cell is $N(N-1)/2$, which can become unacceptably large as the total number of cells increases. Thus, a smaller number of connections is used, and the topology of that balancing network greatly influences the ability of the charge balancing system to maintain an equal state of charge across the pack.

The pack can be represented by a graph, where the nodes of the graph represent the individual cells and the connections between the cells are the edges of the graph. For a battery pack with a charge balancing system two natural graphs can be identified—the first corresponds to the delivery of power by the battery pack and the second represents the charge balancing system itself. The power topology describes the series and parallel combinations that form the battery pack and is typically determined by the load requirements, while the balancing topology is a design variable. It is assumed that each cell will contain some type of control knowledge, and that it can transfer charge to other cells through bidirectional links. Here undirected graphs are used, although directed graphs could be applied if the balancers can only transfer charge in one direction. Finally, the controller design is local in nature, so that the interaction between cells depends only on the charge in the connected cells, and is not specified by a global observer.

This work explores the dynamics of the overall battery pack/charge balancing systems and specifically the influence of the balancing topology design on the overall performance of the charge balancing system. The appropriate model for the battery pack, including the power topology and the individual cell models, is given in Section 2, together with the charge transfer model. In Section 3 appropriate measures of the balancing performance are defined and significant graph characteristics are identified. These ideas are explored in Section 4, as applied an 8-cell pack, with two parallel strings of four cells in series. Finally, concluding remarks are given in Section 5.

2. Model

2.1. Battery pack

Here we consider an $S \times P$ network for the power delivery in the pack, with S cells in series, composing a single strand, and then P strands connected in parallel. The pack illustrated in Fig. 1a would therefore be a 5×4 power network, or a 5S4P network using common notation. The total current and voltage through the pack is given by I_ℓ and V_ℓ respectively, while individual cells are indexed as jk, with $j = 1,\ldots,S$ and $k = 1,\ldots,P$. The quantity I_{jk} represents the current through an individual cell and V_{jk} measures the voltage across the corresponding cell. In terms of the individual cells, the pack current and voltage can be determined as

$$V_\ell = V_k, \quad V_k = \sum_{j=1}^{S} V_{jk}, \tag{1a}$$

$$I_\ell = \sum_{k=1}^{P} I_k, \quad I_{jk} = I_k. \tag{1b}$$

Physically the current through the kth parallel strand is I_k while V_k is the voltage across this strand of cells. This pack is then subjected to an appropriate load characterized as either i) current controlled (I_ℓ = constant), ii) voltage controlled (V_ℓ = constant), or iii) resistive ($V_\ell = R_\ell I_\ell$).

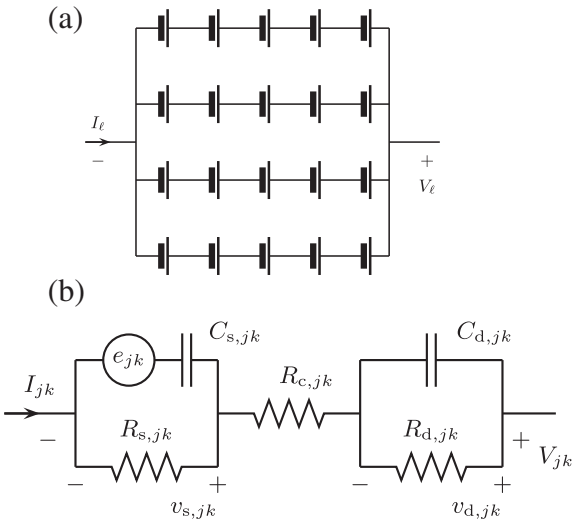

Fig. 1. Battery model; (a) pack power topology, (b) individual cell.

2.2. Cell model

The modeling of individual cells describes the battery performance in terms of, for example, the cell voltage or state-of-charge [10–14]. Individual cells can be represented as shown in Fig. 1b, with the model written as [15]

$$V_{jk} = v_{s,jk} + R_{c,jk}\, I_{jk} + v_{d,jk}, \tag{2a}$$

$$\left(R_{s,jk}C_{s,jk}\right)\frac{\mathrm{d}v_{s,jk}}{\mathrm{d}t} + v_{s,jk} = R_{s,jk}\, I_{jk}, \tag{2b}$$

$$\left(R_{d,jk}C_{d,jk}\right)\frac{\mathrm{d}v_{d,jk}}{\mathrm{d}t} + v_{d,jk} = R_{d,jk}\, I_{jk}. \tag{2c}$$

In the context of this battery system, $v_{s,jk}$, known as the stored voltage, measures the total voltage across the source e_{jk} and the capacitor $C_{s,jk}$, and is identified with the state of charge in the cell—the cell is fully charged when $v_{s,jk} = v_{jk}^{\star}$ and is discharged when $v_{s,jk} = e_{jk}$. The voltage $v_{d,jk}$ represents the diffusing charge in the cell. Also, in typical cells the value of $R_{s,jk}$ is large and influences the self-discharge in the cell, while the resistance $R_{d,jk}$ is typically small, so that the diffusive voltage is likewise small. The resulting model, considering each individual cell together with the topology of the pack, is characterized as a differential-algebraic system of equations for the internal cell states, the current through each series connection of cells, and the voltage across the total pack.

2.3. Charge balancing

As charge balancing is added to the pack, these equations are augmented to represent charge transfer between individual cells. In particular, here we assume that charge transfer occurs through the use of an intermediate transformer. The current through each transformer is denoted as σ_r, which is initially drawn off one cell thus energizing the transformer, as illustrated in Fig. 2. The polarity of the transformer (denoted by the dots in the figure) is such that when the transformer is switched after time T the charge gathered from the previous cell is then transferred to the receiving cell. The resulting model for this process is given as

$$L_{b,r}\frac{\mathrm{d}\sigma_r}{\mathrm{d}t} + R_{b,r}\sigma_r = V_{jk}, \tag{3a}$$

$$I_{jk} = I_k - \sigma_r. \tag{3b}$$

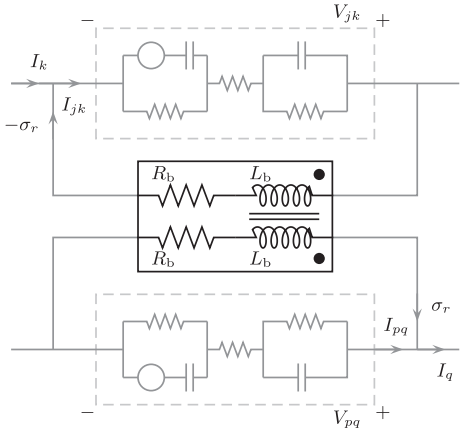

Fig. 2. Charge transfer model. In this figure, charge is transferred from cell jk to cell pq through the transformer.

The charge transfer is active when ever the difference in the voltages between two connected cells exceeds a threshold, identified as δ. If charge is being transferred to a cell, then $\sigma_r \geq 0$ while $\sigma_r \leq 0$ as charge is being transferred from a cell, and diodes are employed within the transformer to enforce these inequalities. With this, the cell current in Eq. (1b) is replaced by Eq. (3b).

Each charge balancing connection adds additional equations of the form of Eq. (3) to the pack model. Typical cell balancing networks are static, so that, for example, cell 12 is connected to cell 52. However, these connections need not follow the topology of the power network. We refer to the topology of the connections associated with the charge balancing as the *balancing network*. This work explores the influence of this balancing on the ability of the charge balancing system to maintain an equal state of charge across each cell in the pack.

The current capacity of the charge balancing system can be defined as the total charge that can be transferred per unit time through the charge balancing system (for a constant voltage difference between cells). With fixed transformer parameters, as the number of connections in the charge balancing system increases, the total charge that can be transferred likewise increases. For an individual transformer, as described in Eq. (3), with a constant switching time and voltage difference across cells, the charge transferred scales inversely with the parameters R_b and L_b. To compare charge balancing networks of differing size, the balancing parameters of individual transformers are scaled according to the total number of transformers, so that the current capacity of the balancing system is constant, even as the number of transformers changes. Specifically, the transformer parameters are scaled as $R_b = \widehat{R}_b/M$ and $L_b = \widehat{L}_b/M$, where the balancing system has M transformers, and $\widehat{R}_b$ and $\widehat{L}_b$ represent nominal values of the transformer parameters. This scaling of the transformer parameters allows for a fair comparison between charge balancing systems that possess different numbers of transformers.

3. Balancing performance and graph properties

The response of the charge balancing system is quantified through the instantaneous maximum voltage difference across the pack, that is

$$\begin{aligned}\Delta(t) &= \max\left\{V_{jk}(t), j\in[1,S], k\in[1,P]\right\} \\ &\quad - \min\left\{V_{jk}(t), j\in[1,S], k\in[1,P]\right\}, \\ &= \left\|V_{jk}\right\|_\infty - \frac{1}{\left\|\frac{1}{V_{jk}}\right\|_\infty}.\end{aligned} \tag{4}$$

In numerical simulations, the voltage difference typically decays in a near-exponential manner for an initial interval, before reaching a nearly constant value after some finite time. Therefore, to evaluate the performance of the charge balancing system, the time-evolution of $\Delta(t)$ is fit to the nonlinear function

$$f(t) = \max\left\{\mathscr{C}_0, f_0\exp\left(\frac{-at}{1-t/b}\right)\right\}, \tag{5}$$

where the parameters $\mathscr{C}_0$, f_0, a, and b are determined through a nonlinear optimization method. This function has been observed to give a reasonable fit to the data. Thus, the quantity $\mathscr{C}_0$ represents the long-term voltage difference, while

$$\mathscr{C}_1 \equiv a + \log(d/\mathscr{C}_0)/b, \tag{6}$$

represents the average exponential decay rate of the voltage difference to this stationary value. The identified parameter f_0

represents the initial unbalance of the pack and thus is not directly correlated to the performance of the charge balancing system.

In addition to the dynamic performance of the battery pack, we can also identify several measures of the underlying graph that is associated with cell connections within the charge balancing system. The diameter d of a graph represents the maximum number of edges between any two individual cells. Smaller diameter graphs require fewer charge balancing steps to transfer charge from one cell in a pack to another. The degree of a node is the number of edges connected to that node. A k-regular graph is defined as one for which the degree of each node is identical, equal to k.

The resiliency of a network can be identified with its ability to operate with acceptable performance under the failure of one or more nodes or edges. One measure of resiliency for a graph is the spectral gap [16], defined as the difference between the largest two eigenvalues of the adjacency matrix A_{rs} of the graph, whose elements are defined as

$$A_{rs} = \begin{cases} 1 & \text{nodes } r \text{ and } s \text{ are connected,} \\ 0 & \text{otherwise.} \end{cases} \tag{7}$$

For a k-regular graph, the largest eigenvalue of A_{rs} is $\lambda_1 = k$ and, with its eigenvalues ordered as $\lambda_1 = k \geq \lambda_2 \geq \cdots \geq \lambda_N$, the spectral gap is identified as $g = k - \lambda_2$.

In this context, the design of a graph for charge balancing in the battery pack requires that for a given number of cells (nodes), we identify graphs that minimize the number of transformers (edges) while minimizing the number of steps required to transfer charge from one arbitrary cell to another (diameter) and maximize the resiliency of the balancing network (spectral gap). This problem is related to the degree-diameter problem in graph theory, which seeks to determine the largest graph with a given degree and diameter. Solutions to this problem are known to be Moore graphs, generalized Moore graphs, or near-Moore graphs. Recently, Donetti et al. [17,18] have introduced a class of graphs, described as *entangled*, characterized as a homogeneous network with an extremely interwoven, or entangled, structure. Moreover, in most cases these networks maximize the spectral gap.

4. 8-Cell network

It is expected that the topology of the underlying charge balancing network will influence the ability of the balancing system to equalize the charge, even though the current capacity is held constant between different charge balancing systems. In what follows, a variety of balancing topologies are chosen to represent graphs with different properties, such as diameter or spectral gap, and the resulting performance of the charge balancing system is simulated and evaluated in terms of the measures $\mathscr{C}_0$ and $\mathscr{C}_1$ defined through Eq. (5).

As an example we consider an 8-cell pack configured in a 4×2 power network. The pack configuration is shown in Fig. 3a and in terms of an undirected graph we represent the pack topology as shown in Fig. 3b. In addition, we assume the nominal parameters for each cell to be

$$\begin{aligned} R_c &= 3.00 \times 10^{-2}\Omega, \quad R_s = 1.00 \times 10^{5}\ \Omega, \quad R_d \\ &= 2.00 \times 10^{-2}\ \Omega, \quad C_s = 1.44 \times 10^{4}\ \text{F}, \quad C_d \\ &= 5.00 \times 10^{3}\ \text{F}, \quad e = 3.00\ \text{V}, \end{aligned} \tag{8}$$

and each is assumed to be fully charged with $v^\star = 4\,\text{V}$, so that $v_{s,jk}(0) = 1\,\text{V}$. With identical parameters and initial state in each cell, the pack will remain balanced as it discharges, so that $V_{jk} = V_\ell/4$ and $I_{jk} = I_\ell/2$. With this ideal configuration $\Delta(t) = 0$. To represent an unbalanced pack, we apply a random variation to the initial charge in each cell, with a maximum variation is no more than 10% of the nominal value $V_{jk}(0) = v^\star$.

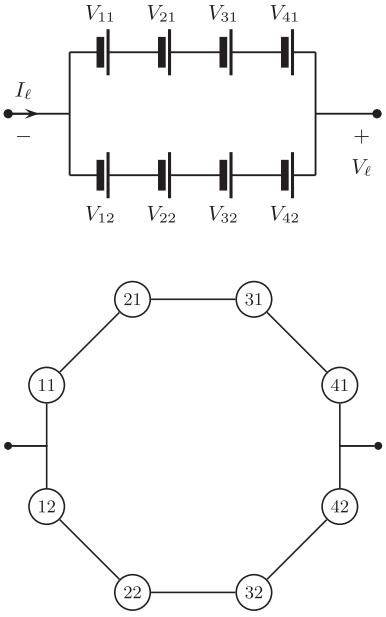

Fig. 3. Battery, 4×2 pack.

These individual parameters approximately correspond to nominal values of $LiCoO_2$ 18650 cells. Finally, the resistive load across the battery pack is assumed to be $R_\ell = 1.00\ \Omega$. While the primary goal of the present study is to address the role of network topology on the performance of charge balancing in battery packs, the 8-cell network is representative of battery requirements in applications such as industrial tools or small robotic vehicles. In such examples four lithium cells can be connected in series to create a pack with a voltage range of roughly 10 V–16 V, which can be used to replace a traditional 12 V lead-acid battery. As is done here, two (or more) such strings can subsequently be connected in parallel to increase the capacity of the pack.

Five different balancing topologies are considered for this 4×2 pack—the case with no balancing and the four additional networks as seen in Fig. 4. In this figure the number of connections, the diameter, and the spectral gap of each graph are indicated in the caption. These four networks represent two common, ordered topologies, a ring whereby each cell is connected to an adjacent cell, and series balancing on each parallel strand in the pack. Finally, two additional networks are identified, chosen specifically for their graph properties. The first is an entangled network with degree 3, while the other is a complete graph, so that each cell is connected to every other cell.

In the context of charge balancing there are typically multiple paths that can be used to move charge from one cell to another. However, recall that despite the different number of connections for each of these graphs, the transformer parameters R_b and L_b are scaled as described in Section 2.3, so that the current capacity of the balancing system in each example is identical. Therefore the average balancing current to an individual cell is independent of the number of connections in the balancing system. It is expected that differences in the performance of these various charge balancing networks should arise from the topology of the network, rather than simply the number of connections or paths between cells.

In the absence of charge balancing, the current in the pack and the voltage in the individual cells are shown in Fig. 5. To highlight

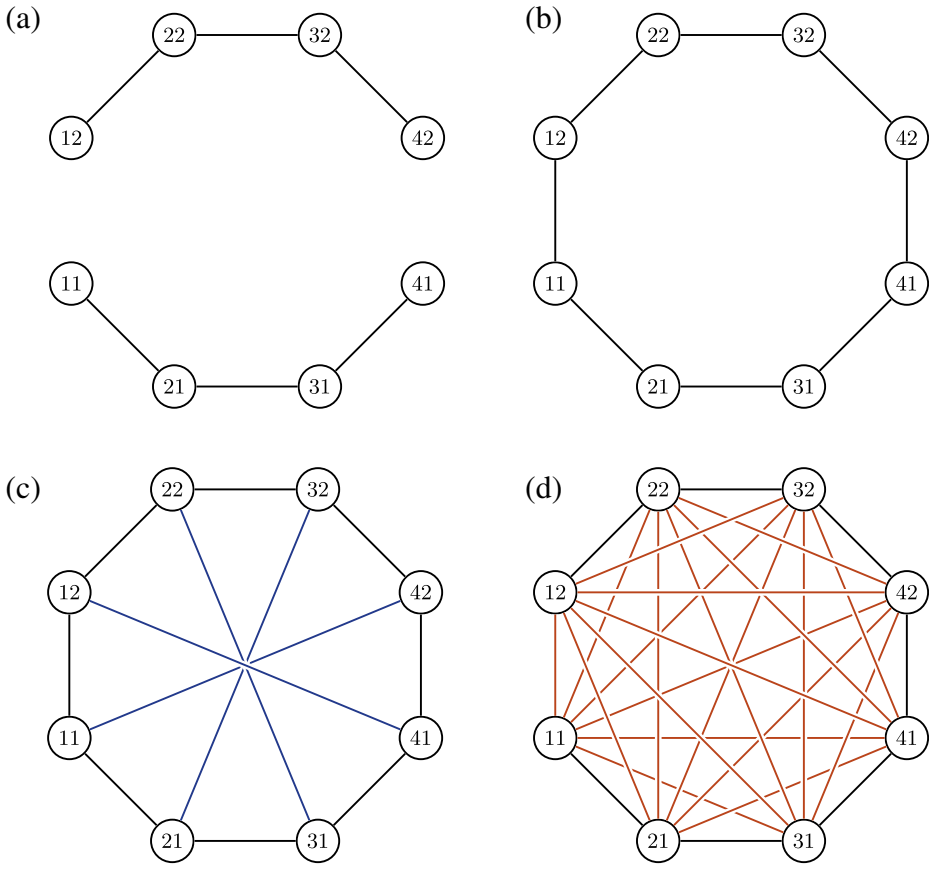

Fig. 4. Balancing network, 4 × 2 pack; (a) series ($M = 6$, $d = \infty$, $g = 0$), (b) ring ($M = 8$, $d = 4$, $g = 0.586$), (c) entangled ($M = 12$, $d = 2$, $g = 2$), (d) complete ($M = 28$, $d = 1$, $g = 8$).

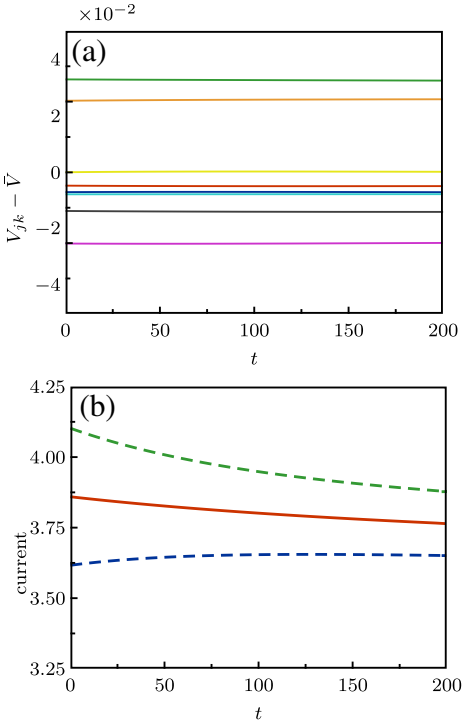

Fig. 5. 4 × 2 pack dynamics, no balancing: (a) voltage unbalance ($V_{jk} - \overline{V}$), the dashed lines are cells in one parallel strand while the solid lines represent the other strand; (b) current, the dashed lines represent the current in each parallel string of cells, while the solid line is the average current. The nominal cell parameters are given in Eq. (8).

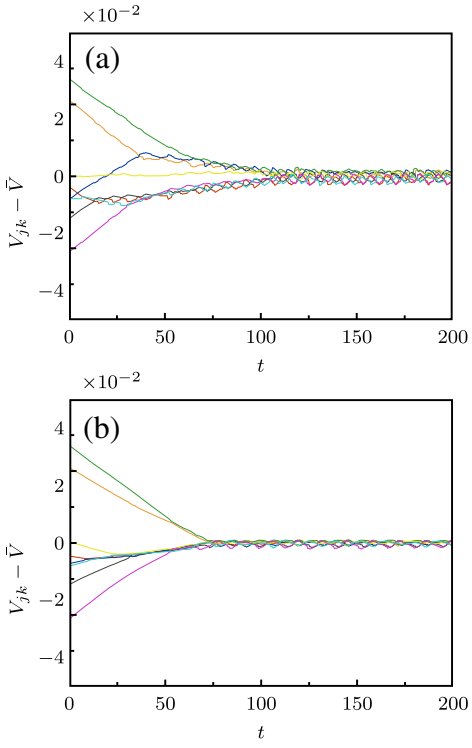

Fig. 6. Cell voltage unbalance ($V_{jk} - \overline{V}$), 4 × 2 pack. The voltage in each individual cell is shown, relative to the mean voltage across the pack; (a) series network, (b) complete network. The nominal cell parameters are given in Eq. (8).

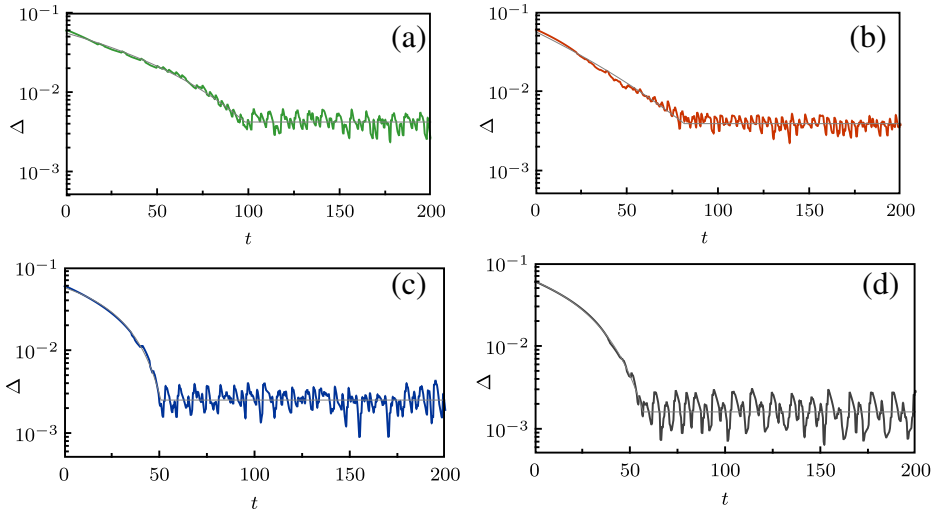

Fig. 7. Pack performance $\Delta(t)$, 4 × 2 pack; (a) series, $\mathscr{C}_0 = 4.19 \times 10^{-3}$, $\mathscr{C}_1 = 2.64 \times 10^{-2}$, (b) ring, $\mathscr{C}_0 = 3.90 \times 10^{-3}$, $\mathscr{C}_1 = 3.28 \times 10^{-2}$, (c) entangled, $\mathscr{C}_0 = 2.47 \times 10^{-3}$, $\mathscr{C}_1 = 6.18 \times 10^{-2}$, (d) complete, $\mathscr{C}_0 = 1.60 \times 10^{-3}$, $\mathscr{C}_1 = 6.39 \times 10^{-2}$. In each panel the nonlinear fit given in Eq. (5) is shown as the thin line. The nominal cell parameters are given in Eq. (8).

the cell unbalance, the mean cell voltage in the pack is identified as $\overline{V}$, and the voltage imbalance in each cell is identified as $V_{jk} - \overline{V}$. In the absence of the charge balancing system the cell voltages remain unbalanced as the pack discharges, as shown in Fig. 5a. In Fig. 5b the current in each parallel strand of cells is shown. Note that the battery topology itself serves to equalize the voltage across any of the parallel strands of cells—the current through each strand ensures that the total voltages are identical. The battery does not serve to balance individual cells, only the total voltage across parallel strands of cells.

The cell voltage is significantly affected by the charge balancing system. With a complete-topology balancing system (c.f. Fig. 4d) the voltage unbalance across the pack decreases as the charge is transferred across the pack, illustrated in Fig. 6. While the charge balancing system brings the individual cell voltages together, because of the localized nature of the connections between individual cells, the voltage imbalances do not simply decay monotonically to their final stationary state. Instead, the balancing system shuttles charge between paired cells and there is no centralized control of the process—the charge synchronization occurs through the localized behavior of the charge balancing system. Note that some difference in voltage between the cells remains due to the threshold δ present for the activation of the balancing between cells and the switching time T associated with the transformers.

For different underlying charge balancing networks the overall performance as measured by $\Delta(t)$ is shown in Fig. 7. While all of the charge balancing systems are able to reduce the unbalance in the pack the time required to do so depends significantly on the balancing topology. Recall that the overall current capacity of the balancing system is held constant for these simulations, so that the performance differences are primarily due to the topology of the balancing connections rather than the total number of connections. The complete graph and the entangled network reach their stationary values much faster than do the ring or series topologies. In addition, these stationary values also depend on the specific balancing network used, with the complete network achieving the smallest imbalance, followed by the entangled graph and the ring and series networks. The stationary imbalance values that arise in the pack can be related to the diameter of the balancing graph d and the balancing threshold δ, which recall represents the voltage difference below which charge is transferred between cells. If the value of Δ is greater than the product $d \cdot \delta$ then charge balancing is guaranteed to occur. Thus, it is expected that balancing networks with lower diameter will lead to lower stationary levels of cell imbalance.

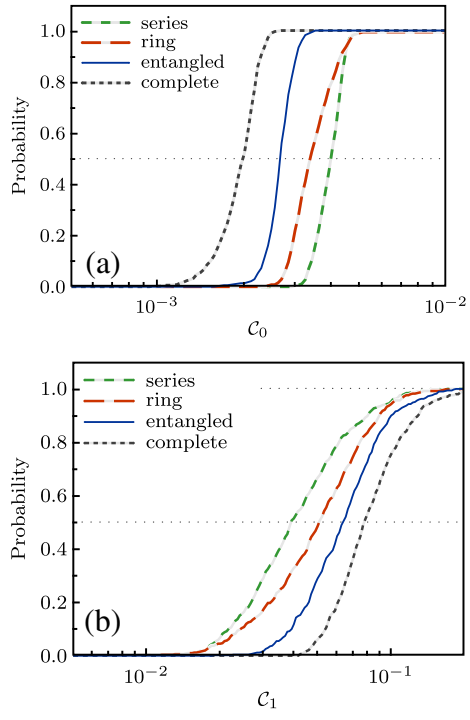

Fig. 8. Probability distribution for the performance, 4 × 2 pack; (a) $\mathscr{C}_0$, (b) $\mathscr{C}_1$. The performance of each network, as listed in Fig. 4 is shown. The nominal cell parameters are given in Eq. (8).

Table 1
Graph properties (d, g) and corresponding balancing performance ($\mathscr{C}_0$, $\mathscr{C}_1$).

	d	g	$\mathscr{C}_0$	$\mathscr{C}_1$
Series	∞	0	3.89×10^{-3}	1.74×10^{-2}
Ring	4	0.586	3.30×10^{-3}	2.30×10^{-2}
Entangled	2	2	2.60×10^{-3}	2.92×10^{-2}
Complete	1	8	1.93×10^{-3}	3.60×10^{-2}

As the initial charge in the pack varies, the performance of the charge balancing system as measured by $\mathscr{C}_0$ and $\mathscr{C}_1$ varies as well. In Fig. 8 the probability distribution of the resulting performance is shown for 512 separate realizations of the initial charge distribution in the pack. This distribution represents the probability that the given measure lies below some value, as listed on the independent axis. For these measures, lower values of $\mathscr{C}_0$ indicate better long-term balancing, while larger values of $\mathscr{C}_1$ indicate faster convergence to this stationary value. The complete network, whereby each cell is connected to every other cell, provides the best performance for the charge balancing system in terms of both $\mathscr{C}_0$ and $\mathscr{C}_1$. The performance measure is worst for the parallel network, illustrated in Fig. 4 where no transfer occurs between parallel connections of cells. Although the complete graph is superior in terms of performance, the number of edges ($M_{\text{complete}} = 28$) far exceeds that of the remaining balancing networks. In particular, the entangled graph provides a good balance between performance and number of connections ($M_{\text{entangled}} = 12$). As noted above the current capacity for each balancing network is identical, so that each balancing system is capable of transferring an equal amount of charge per unit time, alleviating the differences between the number of connections in the different topologies.

From Fig. 8, the long-term performance of the charge balancing system as measured by $\mathscr{C}_0$ can be correlated to the diameter of the underlying graph of the connections—graphs with lower diameter typically provide better balancing performance, requiring fewer charge transfer steps to move energy from one cell in the pack to another. The graph properties and performance metrics for the four networks considered are summarized in Table 1. In this table the values of $\mathscr{C}_0$ and $\mathscr{C}_1$ are evaluated at the 50% probability level from Fig. 8.

5. Summary and conclusions

This paper has presented an initial investigation toward the design of charge balancing systems for advanced battery packs composed of a multitude of individual cells. Specifically, the role of the cell balancing network has been considered, and the topology of the graph underlying this network has been shown to strongly influence the ability of the charge balancing system to equalize the voltages in the individual cells.

Standard charge transfer techniques, such as flying capacitors, suffer from low reliability and long charge transfer paths. Likewise, simple connections based on pack geometry, such as connections to neighbors in a string, can require many charge transfers to balance the pack, and are shown to lead to long equalization times. Likewise, simple geometry-based connections also have low reliability since a broken charge transfer path can lead to extremely long paths or completely isolated cells. Conversely, fully connected packs with all cells connected to all other cells through charge transfer elements, have high reliability and short charge transfer paths, but the large numbers of charge transfer elements are prohibitively expensive and bulky.

This paper has shown an alternative to the structure of battery pack balancing networks, in which the topology of the charge transfer structure is represented by an entangled graph. This network allows for a relatively low number of charge transfer elements as compared to a complete graph, while maintaining good balancing performance and short transfer paths. The entangled graph balancing network thus provides a low cost, reliable alternative to a completely connected graph balancing network, while being only slightly more expensive and much more reliable than a simple geometry-based balancing network. Moreover, this work has developed a framework for evaluating the performance of different balancing topologies and opens the possibility of optimal design of charge balancing systems for advanced battery packs. These ideas have been illustrated through simulations of an 8-cell battery pack. While larger packs used in, for example, electric vehicles will require the use of a larger network of charge-balancing connections, the framework developed here and the methodology used to evaluate the role of the underlying balancing graph will continue to be applicable. Such studies on larger packs, including hardware implementation, are currently under investigation.

References

[1] N.H. Kutkut, D.M. Divan, Dynamic equalization techniques for series battery stacks, in: Eighteenth International Telecommunications Conference (INTELEC), 1996, pp. 514–521.
[2] N.H. Kutkut, H.L.N. Wiegman, D.M. Divan, D.W. Novotny, IEEE Transactions on Aerospace and Electronic Systems 34 (1).
[3] Y.-S. Lee, M.-W. Cheng, IEEE Transactions on Industrial Electronics 52 (5).
[4] M. Einhorn, W. Roessler, J. Fleig, IEEE Transactions on Vehicular Technology 60 (6) (2011) 2448–2457.
[5] S. Yarlagadda, T.T. Hartley, I. Husain, A battery management system using an active charge equalization technique based on a DC/DC converter technology, in: IEEE Energy Conversion Congress and Exposition (ECCE), 2011, pp. 1188–1195.
[6] S.T. Hung, D.C. Hopkins, C.R. Mosling, IEEE Transactions on Industrial Electronics 40 (1) (1993) 96–104.
[7] N.H. Kutkut, D.M. Divan, D.W. Novotny, IEEE Transactions on Industrial Applications 31 (3) (1995) 562–568.
[8] L. Maharjan, S. Inoue, H. Akagi, J. Asakura, IEEE Transactions on Power Electronics 24 (6) (2009) 1628–1636.
[9] C. Pascual, P.T. Krein, Switched capacitor system for automatic series battery equalization, in: Twelfth Annual Applied Power Electronics Conference and Exposition (APEC), 1997, pp. 848–854.
[10] Z.M. Salameh, M.A. Casacca, W.A. Lynch, IEEE Transactions on Energy Conversion 7 (1).
[11] L. Gao, S. Liu, R.A. Dougal, IEEE Transactions on Components and Packaging Technologies 25 (3) (2002) 495–505.
[12] B.Y. Liaw, G. Nagasubramanian, R.G. Jungst, D.H. Doughty, Solid State Ionics 175 (2004) 835–839.
[13] M. Chen, G.A. Rincón-Mora, IEEE Transactions on Energy Conversion 21 (2) (2006) 504–511.
[14] A.A.-H. Hussein, N. Kutkut, B. Issa, A hysteresis model for a lithium battery cell with improved transient response, in: Twenty-Sixth Annual IEEE Applied Power Electronics Conference and Exposition (APEC), 2011, pp. 1790–1794.
[15] R.L.I. Hartman, An Aging Model for Lithium-ion Cells. Ph.D. thesis, The University of Akron, Akron, OH, 2008.
[16] N. Saito, Y. Iba, Computer Physics Communications 182 (1) (2011) 223–225.
[17] L. Donetti, P.I. Hurtado, M.A. Muñoz, Physical Review Letters 95 (2005) 188701.
[18] L. Donetti, F. Neri, M.A. Muñoz, Journal of Statistical Mechanics (2006) P08007.